

Electronic Supplementary Information:

Lipid Vesicles Induced Ordered Nanoassemblies of Janus Nanoparticles

Yu Zhu,¹ Abash Sharma,¹ Eric J. Spangler,¹ Jan-Michael Y. Carrillo,² P.B. Sunil Kumar,³ and Mohamed Laradji^{1,a}

¹*Department of Physics and Materials Science, The University of Memphis, Memphis, TN 38152, USA*

²*Center for Nanophase Materials Sciences, Oak Ridge National Laboratory, Oak Ridge, TN 37831, USA*

³*Department of Physics, Indian Institute of Technology Madras, Chennai 600036, India*

SI. MODEL AND COMPUTATIONAL METHOD

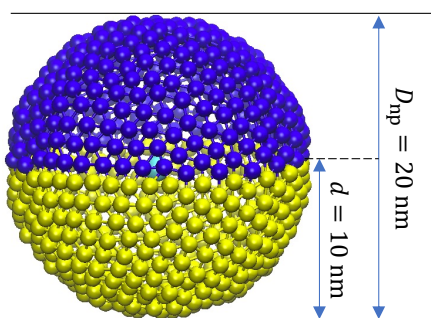


FIG. S1. Configuration of a spherical Janus NP equilibrium with $D = 20$ nm. Only yellow beads are able to adhere to the lipid membrane, the cyan bead is located at the center of NP, and is connected to all other beads by harmonic bonds (not shown for clarity) to maintain a spherical shape of the NP. In this case, the Janusity $J = d/D = 0.5$, where d is the height of the spherical cap that interacts attractively with the lipid head beads.

The bending modulus of the bare membrane, with the interaction parameters given in Table.1 in the manuscript, and as extracted from the spectrum of the height fluctuations of a tensionless bilayer, is $\kappa \approx 30k_B T$ [1], which is comparable to the bending modulus of a DPPC bilayer in the fluid phase [2]. From comparison of the thickness of the present model bilayer in the fluid phase, which is very close to $4r_m$, with that of a typical fluid phospholipid bilayer (≈ 4 nm), the small length scale $r_m \approx 1$ nm. Hence, in this study, all lengths are expressed in nanometers and energies are expressed in $k_B T$.

To determine the adhesion energy density of the NPs on the membrane, simulations of a uniform NP (i.e., a Janus NP with $J = 1$) on a tensionless planar membrane are performed at different values of \mathcal{E} (which corresponds to the minimum of the potential energy between an n_a -bead and an h -bead). The adhesion energy density is then defined as $\xi = |E_{adh}|/A_{adh}$, where E_{adh} is the potential energy between the NP and the membrane and A_{adh} is the area of the

^a mlaradji@memphis.edu

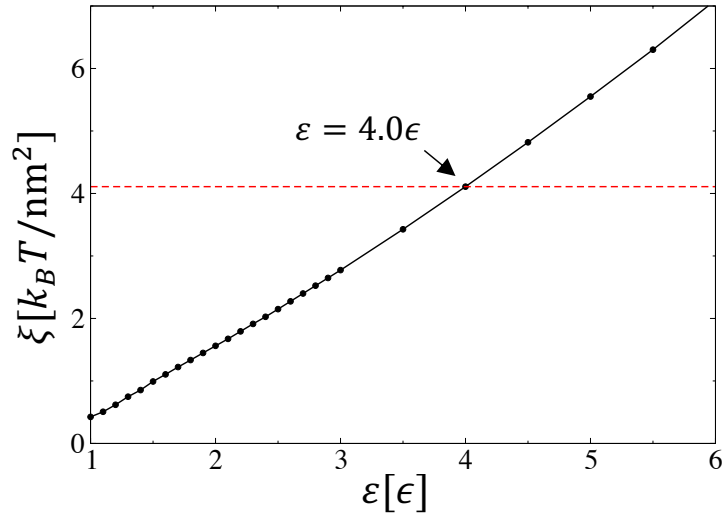


FIG. S2. The adhesion energy density, ξ , versus the interaction strength, \mathcal{E} , between a NP n_a -bead and a lipid h -bead. The red line indicates that the energy density $\xi = 4.11 k_B T / \text{nm}^2$ corresponds to $\mathcal{E} = 4.0\epsilon$.

NP adhering to the membrane. Here, an n_a bead adheres to the membrane if it interacts with at least one h bead of the membrane, i.e. if its distance from the h bead is less than r_c . The dependence of the adhesion energy density ξ on \mathcal{E} in the case of $D = 20$ nm is depicted in Fig. S2. The adhesion energy density in the present study is kept fixed at $\xi = 4.11 k_B T / \text{nm}^2$.

SIII. RADIAL DISTRIBUTION FUNCTION OF UNIFORM NPS

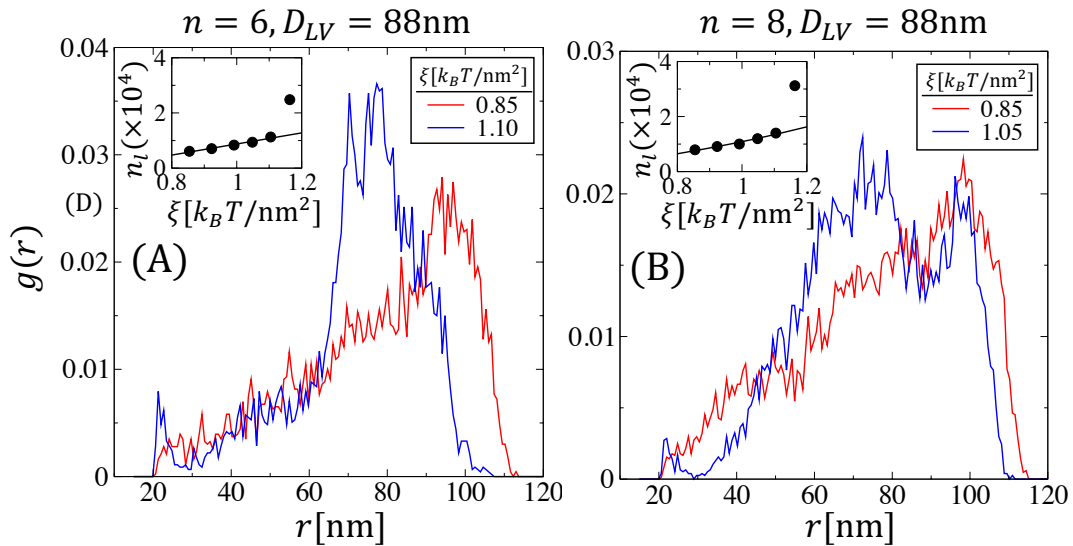


FIG. S3. (A) Radial distribution function, $g(r)$ of the uniform NPs centers of mass at two values of ξ within the gas phase for the case of $n = 6$ and $D_{LV} = 88$ nm. (B) Radial distribution function, $g(r)$ of the uniform NPs centers of mass at two values of ξ within the gas phase for the case of $n = 8$ and $D_{LV} = 88$ nm. Insets of (A) and (B) shows the number of lipid head beads, interacting with the NPs, vs ξ for the same system. The last point in the insets is in the endocytosis phase.

SIII. VESICLES NET AREA VS NUMBER OF JNPS

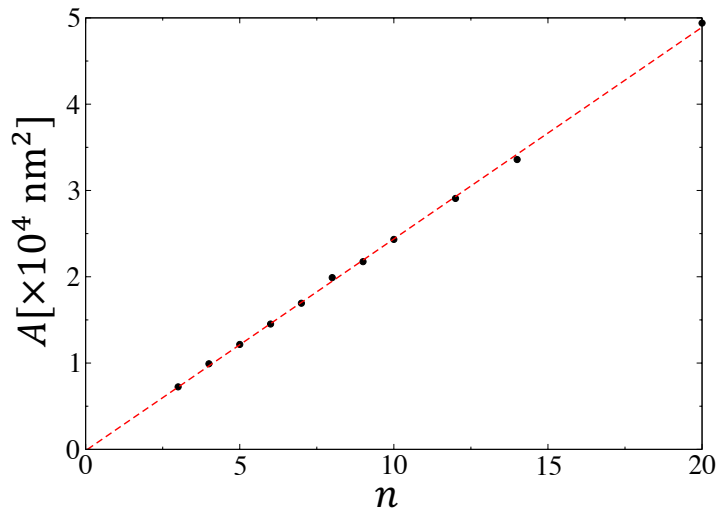


FIG. S4. The surface area of the bare vesicle as a function of the number of NPs adhering to the vesicle. This graph shows that the vesicle size is selected such that the surface area of the vesicle per NP is constant, and equal to $2453 \text{ nm}^2/\text{NP}$.

SIV. BOND ANGLE DISTRIBUTIONS

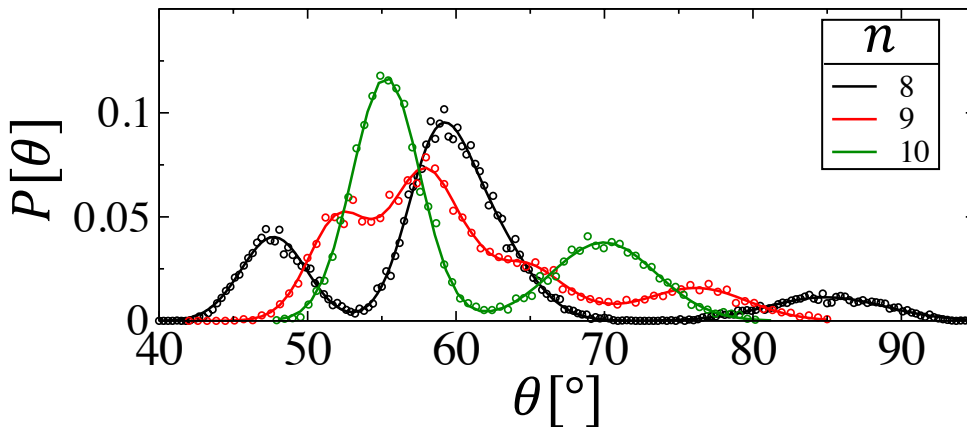


FIG. S5. Bond angle distributions (BDA) for the cases $n = 8, 9,$ and 10 . For $n = 8$, the BDA's best fit is the sum of 4 Gaussians, with peaks at $47.7^\circ, 58.6^\circ, 61.8^\circ$ and 84.4° . For $n = 9$, the BDA's best fit is the sum of 5 Gaussians, with peaks at $52.0^\circ, 57.7^\circ, 60.0^\circ, 62.1^\circ$ and 72.2° . For $n = 10$, the BDA's best fit is the the sum of 2 Gaussians, with peaks at 55.3° and 69.9° .

SV. CONFORMATIONS OF THE VESICLE AND JNPS NANOCCLUSERS IN THE CASES OF 11 AND 13 JNPS

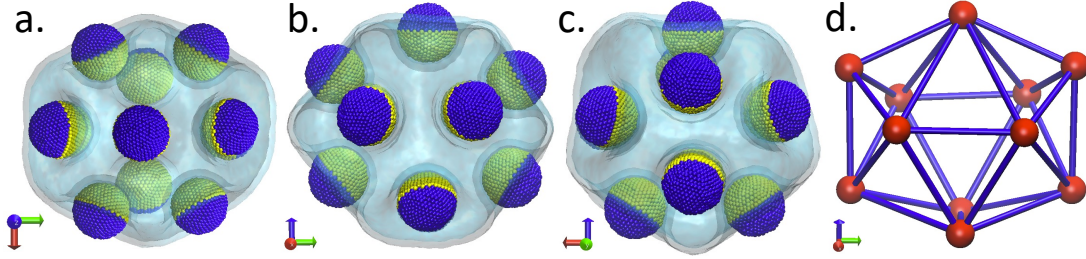


FIG. S6. (a-c) Three views of a vesicle with 11 JNPs. The views are perpendicular to each other. Vesicle and NPs nanocluster conformations in the case of $n = 11$. (d) Snapshot of the NPs with links obtained from spherical Delaunay triangulation [3].

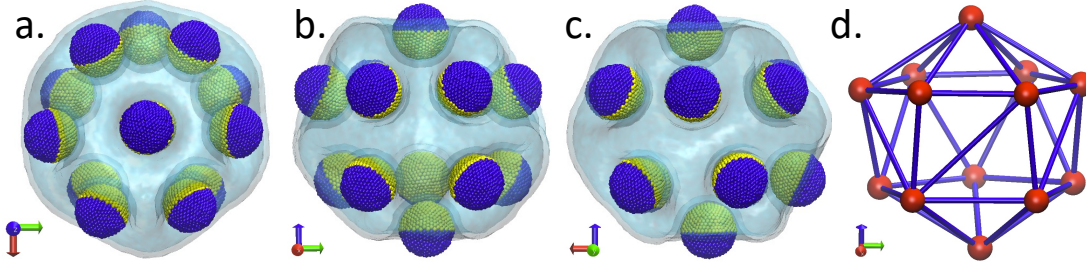


FIG. S7. (a-c) Three views of a vesicle with 13 JNPs. The views are perpendicular to each other. Vesicle and NPs nanocluster conformations in the case of $n = 13$. (d) Snapshot of the NPs with links obtained from spherical Delaunay triangulation [3].

SVI. VESICLE'S CURVATURE ENERGY CALCULATION

To calculate the curvature energy of a vesicle, we use a local Monge representation of the Helfrich Hamiltonian [4]. This is a valid approach since the Helfrich Hamiltonian is invariant under an arbitrary rotation. Our calculation of the free energy is achieved as follows (see Fig. S8) [5]:

- 1) For each lipid i , all neighboring lipids within the same leaflet and within a range $\lambda = 0.865r_m$ are identified, and their average normalized end-to-end vector, $\hat{\mathbf{n}}_i$, is calculated.
- 2) A unit vector, tangent to the membrane at lipid i , $\hat{\mathbf{t}}_i = \hat{\mathbf{n}}_i \times \hat{\mathbf{z}}$, is calculated.
- 3) The portion of the membrane, composed of all lipids within the distance $3\sqrt{2}\lambda$ from lipid i and belonging to the

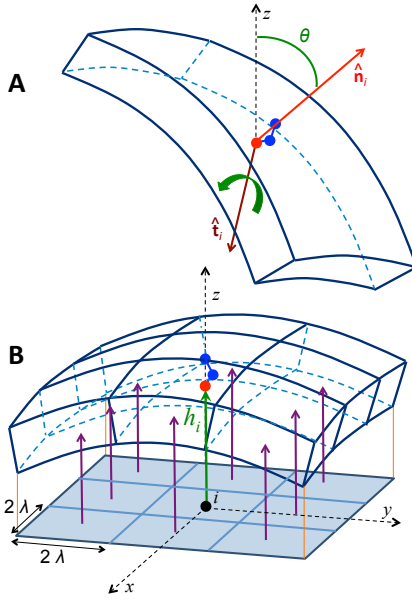


FIG. S8. A schematic representation of a portion of the lipid bilayer, centered at lipid i before rotation (A) and after rotation (B). In (A), $\hat{\mathbf{n}}_i$ is a unit vector in the direction of the mean of the end-to-end vectors of lipids in a small region around i as explained in the text. $\hat{\mathbf{t}}_i = \hat{\mathbf{n}}_i \times \hat{\mathbf{z}}$ is a local tangent vector that is normal to both the z -axis and \mathbf{n}_i . The bilayer is rotated around the vector \mathbf{t}_i by the angle θ between \mathbf{n}_i and the z -axis. Note that the bilayer is not discretized before rotation. The discretized xy -plane in (B) is parallel to the tangent plane to the membrane at i . The vertical purple arrows indicate the heights of the discretized parts of the leaflet, containing lipid i . From Spangler *et al.* [5].

same leaflet, is then rotated around the tangent vector $\hat{\mathbf{t}}_i$ by the angle $\theta = \cos^{-1}(\hat{\mathbf{z}} \cdot \hat{\mathbf{n}}_i)$, using the following matrix [6],

$$\mathbf{R} = \begin{bmatrix} t_{i,x}^2(1-c) + c & t_{i,x}t_{i,y}(1-c) - t_{i,z}s & t_{i,x}t_{i,z}(1-c) + t_{i,y}s \\ t_{i,x}t_{i,y}(1-c) + t_{i,z}s & t_{i,y}^2(1-c) + c & t_{i,y}t_{i,z}(1-c) - t_{i,x}s \\ t_{i,x}t_{i,z}(1-c) - t_{i,y}s & t_{i,y}t_{i,z}(1-c) + t_{i,x}s & t_{i,z}^2(1-c) + c \end{bmatrix} \quad (\text{A1})$$

where $t_{i,x}$, $t_{i,y}$ and $t_{i,z}$ are the components of the unit tangent vector $\hat{\mathbf{t}}_i$, $c = \cos \theta$ and $s = \sin \theta$. The z -axis is now locally normal to the region of the membrane around lipid i .

4) The tangent plane to the rotated portion of the leaflet around lipid i is then discretized into squares of area $a_p = (2\lambda)^2$, such that the projection of lipid i 's head group is at the center of its projection square, as shown by Fig. S8 (B).

5) The local heights of the leaflet in the neighborhood of i is calculated from this reference plane. Partial derivatives $h_{i,\bar{x}}$, $h_{i,\bar{y}}$, etc. are then calculated using the finite difference method involving both nearest and next-nearest neighbors.

The local extrinsic curvature of the leaflet at lipid i is then approximated by,

$$K_i = \frac{(1 + h_{i,\bar{y}}^2) h_{i,\bar{x}\bar{x}} + (1 + h_{i,\bar{x}}^2) h_{i,\bar{y}\bar{y}} - 2h_{i,\bar{x}}h_{i,\bar{y}}h_{i,\bar{x}\bar{y}}}{(1 + h_{i,\bar{x}}^2 + h_{i,\bar{y}}^2)^{3/2}}, \quad (\text{A2})$$

which is then used to calculate the curvature energy of the bilayer

$$E_c = \frac{\kappa}{4} \sum_{i=1}^{N_{\text{lip}}} \Delta\mathcal{A}_i K_i^2. \quad (\text{A3})$$

The denominator 4 in the expression above arises from the fact that the curvature energy is calculated for each leaflet separately, with κ being the bending modulus of the bilayer. The leaflet area, associated with lipid i , in Eq. (A3) is given by

$$\Delta\mathcal{A}_i = \frac{a_p (1 + h_{i,x}^2 + h_{i,y}^2)^{1/2}}{n_i}, \quad (\text{A4})$$

where n_i is the number of lipids whose projection fall onto the local square centered at i . For validation of this approach, we calculated the curvature free energies of spherical vesicles, and found that they are indeed equal to $8\pi\kappa$ within an error less than 5% [5].

SVII. ADHESION AND CURVATURE ENERGIES VERSUS NUMBER OF JNPS

TABLE S1. Excess curvature energy, ΔF_c and adhesion energy, F_a , of the vesicle with JNPs for different values of n . Here $\Delta F_c = F_c - F_c^{(0)}$ where F_c is the curvature energy of the vesicle with adhering JNPs and $F_c^{(0)}$ is the curvature energy of the bare vesicle with same size.

n	$\Delta F_c [k_B T]$	$F_a [k_B T]$	$\Delta F [k_B T]$	$\Delta F_c/n [k_B T]$	$F_a/n [k_B T]$	$\Delta F/n [k_B T]$
3	2039	-8857	-6818	680	-2952	-2273
4	2837	-12490	-9653	709	-3124	-2413
5	3483	-15790	-12307	697	-3158	-2461
6	3403	-19150	-15747	567	-3192	-2625
7	4452	-22340	-17888	636	-3191	-2555
8	4572	-25610	-21038	572	-3201	-2630
9	4646	-28810	-24164	516	-3201	-2685
10	5294	-32060	-26766	529	-3206	-2677
12	6540	-38510	-31970	545	-3210	-2664
14	7472	-44960	-37488	534	-3211	-2678

SVIII. DEGREE OF DISTORTION

The degree of distortion, $\Delta\theta$, of the geometry of the NPs cluster polyhedron from its corresponding deltahedron is defined from the deviation of the bond angles from their average value, i.e.,

$$\Delta\theta = \sqrt{\langle(\theta - \langle\theta\rangle)^2\rangle}, \quad (\text{A5})$$

For all values of n , $\langle\theta\rangle = 60^\circ$. We note that this definition is strictly valid only for those structures which do have corresponding deltahedra, i.e. $n = 4, 5, 6, 7, 8, 9, 10$ and 12 . The values of $\Delta\theta$ vs. n are shown in Table S2.

TABLE S2. Degree of distortion of the bond angle for different values of n .

n	3	4	5	6	7	8	9	10	11	12	13	14	20
$\Delta\theta$	0.475	0.591	6.875	1.860	6.136	10.446	8.047	7.456	7.959	2.324	8.850	5.158	9.379

SIX. RADIAL DISTRIBUTION FUNCTION OF 4 JNPS ADHERING TO A LARGE VESICLE

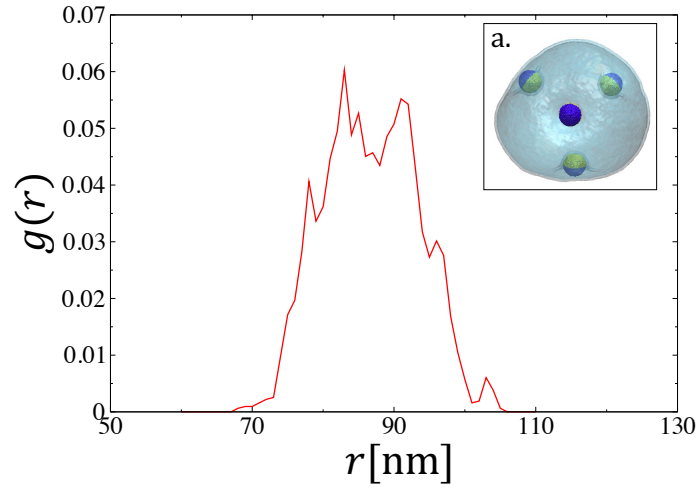


FIG. S9. The radial distribution function for the tetrahedron at $\xi = 4.11k_B T/\text{nm}^2$ and $D_{LV} = 142.4 \text{ nm}$.

SX. RADIAL DISTRIBUTION FUNCTION OF 4-JNPS NANOCCLUSERS WITH DIFFERENT VALUES OF THE JANUSITY

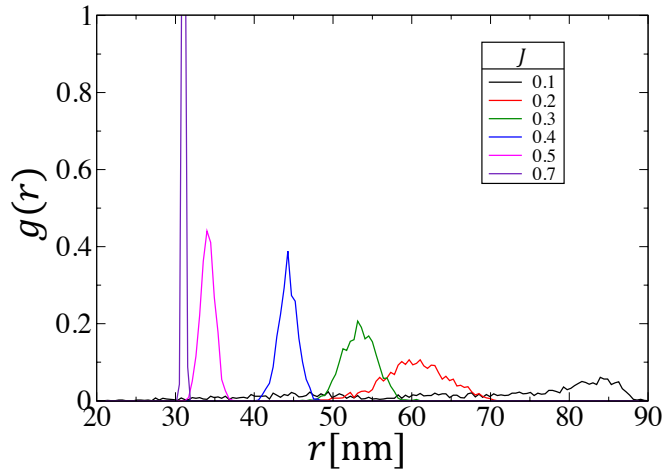


FIG. S10. The radial distribution function of different Janusity for the tetrahedron at $\xi = 4.11k_B T/\text{nm}^2$ and $D_{LV} = 68$ nm.

SXI. RADIAL DISTRIBUTION FUNCTION OF 20-JNPS CLUSTER

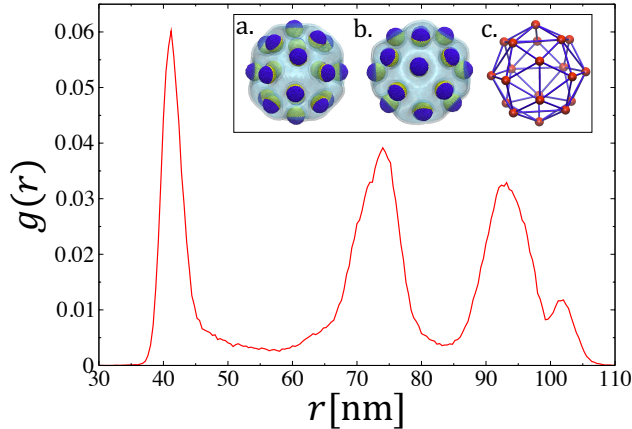


FIG. S11. Radial distribution function in the case of 20 JNPs with $D_{LV} = 127$ nm. Inset: (a) and (b) correspond to two perpendicular views. (c) corresponds to the JNPs nanocluster. The blue links are obtained from a spherical Delaunay triangulation of the structure.

SXII. RADIAL DISTRIBUTION FUNCTION OF A 32-JNPS CLUSTER

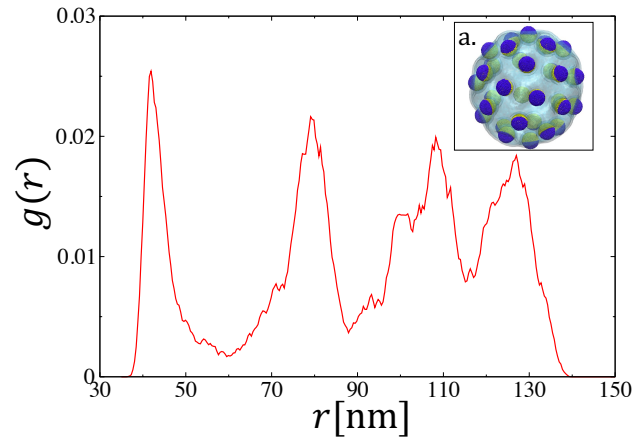


FIG. S12. Radial distribution function in the case of 32 JNPs with $D_{LV} = 158$ nm. Inset is a configuration of then cluster at equilibrium state.

-
- [1] M. Laradji, P. B. Sunil Kumar, and E. J. Spangler, *Journal of Physics D: Applied Physics*, **49**, 293001 (2016).
- [2] J. F. Nagle, M. S. Jablin, S. Tristram-Nagle, and K. Akabori, *Chem. Phys. Lipids* **185**, 3 (2015).
- [3] M. Caroli, P. M. M. de Castro, S. Lorient, O. Rouiller, M. Teillaud, and C. Wormser, in *Experimental Algorithms*, edited by P. Festa (Springer Berlin Heidelberg, Berlin, Heidelberg, 2010) pp. 462–473.
- [4] W. Helfrich, *Z. Naturforsch. C: J. Biosci.* **28**, 693 (1973).
- [5] E. J. Spangler, P. B. Sunil Kumar, and M. Laradji, *Soft Matter* **14**, 5019 (2018).
- [6] P. D. Lin, *Advanced Geometrical Optics* (Springer, 2017).